Electric Power Systems Research 165 (2018) 238–249

Contents lists available at ScienceDirect

Electric Power Systems Research

journal homepage: www.elsevier.com/locate/epsr

Selectivity and security of DC microgrid under line-to-ground fault

R. Lazzari[a], L. Piegari[c], S. Grillo[c,*], M. Carminati[b], E. Ragaini[b], C. Bossi[a], E. Tironi[c]

[a] RSE, Ricerca sul Sistema Energetico, via R. Rubattino 54, I-20134 Milano, Italy
[b] ABB, SACE Division, via Pescaia, 5, I-24123 Bergamo, Italy
[c] Politecnico di Milano, Dipartimento di Elettronica, Informazione e Bioingegneria, p.zza Leonardo da Vinci, 32, I-20133 Milano, Italy

ARTICLE INFO

Keywords:
Dc ground fault
Dc microgrids
Line-to-ground fault protection
Power system protection
Fault selectivity

ABSTRACT

Over the recent years, low-voltage dc (LVDC) distribution systems have become increasingly interesting. One of the main problems in their diffusion is the realization of reliable protection systems ensuring selectivity and security to the loads. Several solutions to this problem are studied in the current literature and are mainly focused on the design and integration of new protection devices. Nevertheless, for some faults, it is possible to use traditional protection devices if proper control strategies are used on the power converters. In this paper, the ground fault of one of the dc poles is considered for grids operated with the neutral ground connected on the ac side and isolated on the dc side. In these conditions, if, as usual, a voltage source converter (VSC) is used as an interface between ac and dc grids, the IGBTs of the VSC are capable neither of limiting nor of blocking the fault current. In this paper, the integration of a proper control strategy implemented on the VSC with the protection devices is proposed to allow the system to interrupt, clearing the fault, saving the power converter. The proposed strategy ensures selectivity and security to the loads because it implies the interruption only of the faulty feeder of the dc microgrid. In this paper, the proposed strategy is tested by means of numerical simulations and experimental results, thus proving its good performances.

1. Introduction

Technological progress, especially in the power conversion field, is fostering the implementation of dc distribution grids [1–3]. This is a growing trend, mainly with sensitive loads [4], distributed generation [5], and electrical vehicle charging stations [6]. DC grids offer several advantages compared with ac in many applications (e.g., data centers, marine installations, offshore wind farms, etc.) and, in particular, in low-voltage distribution grids with a high penetration of distributed energy resources and storage systems.

The implementation of such networks introduces a complex mix of dc and ac grids with significant technical challenges in the development of protection schemes. Moreover, the devices that make up the microgrids and the ground connection of the live parts [7] strongly influence system behavior under fault conditions (both types of fault and fault currents magnitude). Although the protection of microgrids in the case of ac-side faults is not trivial—but can be realized acting on the front-end converter (FEC) control [8]—dc-side faults require different considerations and new challenges.

Several authors have started to deal with these issues, but this topic surely requires further consideration. A fault in a dc grid causes the discharge of the converter capacitors with a current surge that depends only on the filter design, the location of the fault, and the installed capacity of the converter [9]. This also brings current feeding from the ac grid or generation source, without any limitation, through the freewheeling diodes of the voltage source converter (VSC), which acts as a rectifier [10]. Usually, FECs are used also to limit the current, but, if they are VSCs, this is possible only for currents generated on the ac side. In this case, if the fault is on the ac side, the VSC can limit and/or stop the fault current. On the contrary, if the fault is on the dc side, in both cases of pole-to-pole and pole-to-ground faults, the VSC can neither limit nor stop the fault current [7,11,12].

Starting from the analysis of fault current characteristics, the authors in [13] state that fault detection, as performed in ac systems, is not effective in dc microgrids. Thus, traditional protection devices (e.g., directional relays and distance protection) should be adapted in order to be adequate and effective in the new context. Furthermore, the coordination of current-based protection devices is a challenging task, due to the high rising rate of dc fault currents.

DC microgrids protection involves many challenges linked to personal safety, fault detection and location capabilities, equipment survivability, and ride-through capability [14]. The traditional protection

* Corresponding author.
E-mail addresses: riccardo.lazzari@rse-web.it (R. Lazzari), luigi.piegari@polimi.it (L. Piegari), samuele.grillo@polimi.it (S. Grillo), marco.carminati@it.abb.com (M. Carminati), enrico.ragaini@it.abb.com (E. Ragaini), claudio.bossi@rse-web.it (C. Bossi), enrico.tironi@polimi.it (E. Tironi).

https://doi.org/10.1016/j.epsr.2018.09.001
Received 9 February 2018; Received in revised form 4 July 2018; Accepted 2 September 2018

device for a dc microgrid is the ac circuit breaker (ACCB), which acts to isolate the ac source from the fault. However, the trip of the ACCB causes the complete shutdown of the dc link, and the long interruption time does not ensure protection of the VSC. To reduce the dc grid outage time, it is possible to integrate the system with dc protection strategies, e.g., the progressive protection strategy (PPS) algorithm presented in [15]. However, the ACCBs are not fast enough to prevent damages of the components of the dc grid. To prevent damages and to promptly isolate a fault from the grid, the authors in [16] propose the use of fast-acting fuses to replace no-fuse circuit breakers at some certain locations in the dc system. Fast-acting fuses are able to protect a dc microgrid with short critical fault clearing time and are cost effective but cannot be automatically restored after the fault, causing an outage in the faulty part of the grid.

To solve this drawback, some authors propose the use of a dc solid-state circuit breaker (SSCB) to fast detect and isolate a fault. The use of a semiconductor switch connected in series with the capacitor of the dc link [17] can limit the fast rising discharge current, but this solution affects the voltage of the dc grid with power quality issues. To provide a high power quality level also in presence of a fault, the authors in [18] suggest the use of a ring-type low-voltage dc (LVDC) distribution system in which an IGBT circuit breaker is installed at the terminal point of each line. This solution guarantees fast switching speed and high withstanding capability against short circuit currents, but the use of IGBT causes the increase of energy losses. To reduce losses, the authors in [19] proposed a combination of SSCB and hybrid circuit breaker (HCB) to protect a multi-terminal dc compact node. In particular, SSCBs are used to protect each converter capacity filter, while the HCB, which presents lower losses compared with the SSCB, externally protects the grid.

Other useful solutions for the overcurrent protection can be achieved with hardware modification of the power electronics converters. To isolate the power supply devices from the fault, in [20] the authors propose the replacement of the freewheeling diodes of the VSC with other IGBTs and the design of smoothing the capacitor branch. In this way, it is possible to limit the faulty current in a fast way, but new challenges in the development of the protection scheme, which is able to detect and locate faults, emerge. In this situation, the introduction of centralized [21–23] or decentralized [24] control schemes designed to operate (traditional or innovative) protection devices installed in the (potentially meshed) dc microgrid can provide the detection of the fault and the isolation of the faulted section, so that the system keeps operating without disabling the entire system.

The grounding scheme in a dc microgrid is one of the most important issues for the system safety and the protection. The dc grounding options [25] can be classified into four types, i.e., the ungrounded system, the low-resistance grounded system, the high-resistance grounded system, and the solidly grounded system. Compared with other grounding methods, the ungrounded dc system has better continuity of power supply, lower ground leakage current, simpler implementation, and lower installation cost. During a line-to-ground fault, the dc system continues to operate, and only a second ground fault can cause a line-to-line fault [23].

However, in the case of a hybrid ac-dc network in which the neutral point of the ac grid is grounded (on the MV/LV transformer), the occurrence of a line-to-ground fault on the dc side causes a zero-sequence current provided by the ac grid. This current cannot be controlled by IGBT-based VSCs that feed the dc microgrid. The use of an isolating transformer between the MV/LV transformer and the FEC is a good and common solution for solving this problem and to eliminate the injection of dc current [26]. However, this component increases the inverter final cost, its size and weight, and causes higher energy losses. In the same manner, the use of SSCB and HCB or the hardware modification of the power electronic converters increase the final cost and the energy losses.

To solve this problem, the authors in [27] propose the use of a suitable resistance, inserted in series with the protective earthing (PE) conductor, to limit the line-to-ground fault current. The authors also proposed a possible control strategy for the zero-sequence current to protect the FEC during this fault condition without further analysis about the protection of an LVDC microgrid. Moreover, with applying this control strategy, the FEC is protected against the pole-to-ground fault, but this can cause the outage of the overall dc grid.

This paper analyzes the problem of line-to-ground fault and proposes a methodology to ensure the reliability of the LVDC microgrid, resorting to a completely decentralized protection structure that does not require a communication level. The proposed protection structure combines the zero-sequence current control strategy of the FEC with differential circuit breakers and energy storage systems to guarantee the selectivity and the continuity of the service. When a ground fault is detected, the FEC stops supplying the load and starts sustaining the passage of the zero-sequence fault current. Differential circuit breakers installed at the different feeder bays check the unbalance in the current entering and leaving the feeders. Thus, it can detect which feeder is affected by the fault. In this way, only the feeder affected by the ground fault is disconnected. If the feeders are equipped with storage devices, all loads continue to be fed (even those connected to the feeder affected by the fault, as the reclosing path is interrupted by the circuit breakers). When the ground fault is cleared (either by the permanent trip of the feeder's circuit breakers or by autonomous clearance), FEC operation can be restored to normal operating condition. The control strategy and the protection selectivity principle have been validated through field tests using a dc microgrid at RSE.

The paper is structured as follows. Section 2 is dedicated to the description of the control strategy and of the protection selectivity criterion. In Section 3, the test facility used for field verification is described. Results and comments on simulation and field tests are reported in Section 4. Finally, in Section 5 conclusions are drawn.

2. Control strategy and protection selectivity

2.1. Motivation

In large dc grids, several feeders can start from the interconnection point with the ac mains. Usually, the interconnection between the two grids is made with a traditional three-phase, two-level VSC connected to the low-voltage ac grid with or without the interposition of a transformer [3]. For safety reasons, the low voltage ac grid has a WYE configuration with the neutral point connected to the ground. Fig. 1 shows a possible schematic of the system under analysis.

In such a grid, a line-to-ground fault implies a closure path for the fault current involving both ac and dc grids, including the power converter. This current can break the power converter with a consequent blackout on the dc grid if generators and storage are not able to supply it autonomously. Note that the power converter could limit the current only when the dc voltage is higher than the maximum voltage of the ac side.

In order to protect the inverter, in the case of ground fault on the dc side, a control strategy has been proposed and analyzed in [27]. The only aim of this control strategy was to safeguard the power converter. This paper will show how the grid must be modified and how the control strategy can be adapted to ensure the continuity of service to dc loads. In particular, a general dc grid with several feeders will be taken into account, and the control strategy will be integrated with protection devices to allow the continuity of services. Furthermore, a grid configuration will be also proposed to allow the supply of the loads connected to the feeder in which the fault effectively occurs. In order to simplify this paper for the readers, a reminder to the control strategy will be reported here.

It is worth noting that there can be two operating conditions for a microgrid: connected or not with a grid. If the microgrid is in island operation, there is no path for the fault current that involves the FEC,

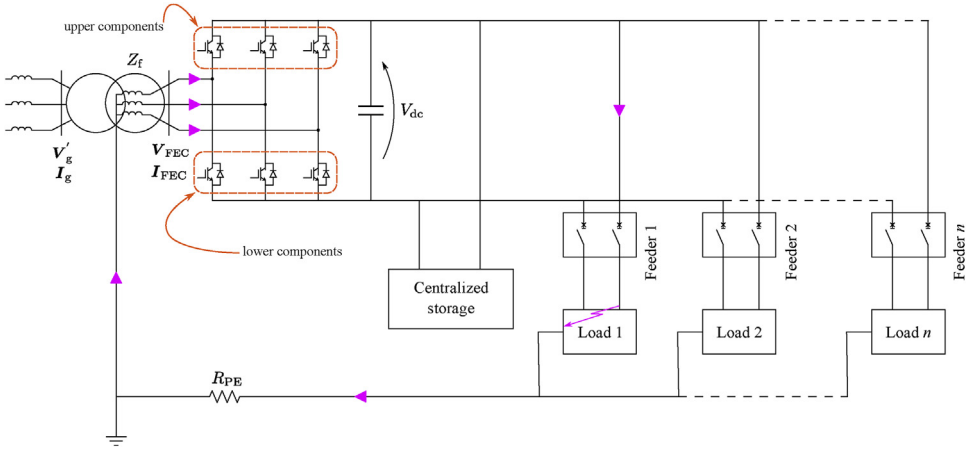

Fig. 1. Simplified schematic of a general dc micro-grid configuration.

and the proposed methodology is not needed. If it is connected, there are two possibilities: either the main grid is able to supply a fault current, which exceeds the maximum current that the FEC can sustain, or the main grid has a low short circuit power resulting in a low ground fault current that could flow for a long time through the FEC (in the limit case even indefinitely). In both cases, the proposed methodology can be applied to protect the microgrid. It is worth noting that the latter case is less demanding than the former.

2.2. Control strategy

When a ground fault occurs on the dc side, a zero-sequence current closes between ac and dc grids across the FEC. The path of the fault current is highlighted in Fig. 1. The zero-sequence current is composed by a continuous component and high-frequency components (around the switching frequency). Obviously, the FEC cannot control the current at switching frequency. Anyway, this current is strongly limited by the inductance of the output filter used to connect the FEC to the ac grid. For this reason, only the continuous component of the zero-sequence current will be taken into account. The converter could be controlled to interrupt the continuous component of the fault current, but it should always keep turned on the three upper (lower) components if the fault involves the positive (negative) line of the dc grid. This configuration is not viable because it causes the short circuit of the ac grid on the converter and the consequent breaking of the FEC.

The main goal of the control strategy is to protect the FEC, which minimizes the current through it during the fault. The space vectors of the inverter, grid voltages, and current are

$$\begin{aligned} \boldsymbol{V}_{\mathrm{FEC}} &= \tfrac{2}{3}\textstyle\sum_{k=1}^{3} v_{\mathrm{FEC},k}(t)\exp\left(j\frac{2\pi(k-1)}{3}\right) \\ \boldsymbol{I}_{\mathrm{FEC}} &= \tfrac{2}{3}\textstyle\sum_{k=1}^{3} i_{\mathrm{FEC},k}(t)\exp\left(j\frac{2\pi(k-1)}{3}\right), \\ \boldsymbol{V'}_{\mathrm{g}} = n\boldsymbol{V}_{\mathrm{g}} &= \tfrac{2}{3}\textstyle\sum_{k=1}^{3} v_{\mathrm{g},k}(t)\exp\left(j\frac{2\pi(k-1)}{3}\right) \end{aligned} \tag{1}$$

where subscripts "FEC" and "g" are used to indicate converter and grid quantities, $k = 1, 2, 3$ is the subscript indicating the three phases, and n is the transformer ratio. Neglecting the high-frequency components and remembering that, during the fault, continuous zero-sequence currents and voltage arise the space vectors defined in Eq. (1) can be written as sum of the first harmonic component (indicated with subscript "a") and of the zero-sequence component (indicated with subscript 0). Taking into account that the alternating component is still a vector, while the zero-sequence component is a scalar, the result is as follows:

$$\begin{aligned} \boldsymbol{V}_{\mathrm{FEC}} &= \boldsymbol{V}_{\mathrm{FEC},a} + V_{\mathrm{FEC},0} \\ \boldsymbol{I}_{\mathrm{FEC}} &= \boldsymbol{I}_{\mathrm{FEC},a} + I_{\mathrm{FEC},0} \\ \boldsymbol{V}_{\mathrm{g}} &= \boldsymbol{V}_{\mathrm{g},a} + V_{\mathrm{g},0} = \boldsymbol{V}_{\mathrm{g},a} \pm \tfrac{V_{\mathrm{dc}}}{2} \end{aligned} \tag{2}$$

The zero-sequence component of the grid voltage is not, properly, in the grid voltage but arises from the modulation of the power converter and is, therefore, equal to half the dc voltage with the plus or minus sign depending on the dc line where the fault occurred. In the VSC, the positive and negative dc poles have, respectively, a positive and a negative voltage potential with respect to the neutral point of the ac source. This voltage has a constant component equal to half of the dc bus voltage and oscillating components at third harmonics and around the switching frequency. This voltage, being the same for the three phases, is a zero-sequence component. This results directly from the theory of VSCs [28,29]. In the present paper, we focus on the dc component of this zero-sequence voltage because the high-frequency components are filtered by the inductive filter of the FEC, while the dc component is only limited by resistances [29]. Let $\dot{Z}_f$ be the sum of the impedances of the inductive filter and of the transformer at the fundamental frequency. Thus, $\boldsymbol{I}_{\mathrm{FEC}}$ can be expressed as

$$\begin{aligned} \boldsymbol{I}_{\mathrm{FEC}} &= \boldsymbol{I}_{\mathrm{FEC},a} + I_{\mathrm{FEC},0} \\ &= \tfrac{\boldsymbol{V}_{\mathrm{FEC},a} - \boldsymbol{V}_{\mathrm{g},a}}{\dot{Z}_f} + \tfrac{V_{\mathrm{FEC},0} \mp V_{\mathrm{dc}}/2}{3R_{\mathrm{PE}} + R_f} \end{aligned} \tag{3}$$

in which R_f indicates the resistive part of $\dot{Z}_f$ and R_{PE} is the intentional resistance inserted in series to the PE conductor. In order to keep the FEC in linear modulation, its maximum output voltage is half the dc voltage. During the fault, the FEC is used at its limit, so it results as follows:

$$V_{\mathrm{FEC},0} = \mp\left(\frac{V_{\mathrm{dc}}}{2} - |\boldsymbol{V}_{\mathrm{FEC},a}|\right). \tag{4}$$

To minimize the current in the FEC, it is clear that the alternating component of the FEC voltage must be in phase with the alternating component of the grid voltage. In this hypothesis, taking into account Eq. (4), Eq. (3) can be rewritten as

$$|\boldsymbol{I}_{\mathrm{FEC}}| = \frac{|\boldsymbol{V}_{\mathrm{FEC},a} - \boldsymbol{V}_{\mathrm{g},a}|}{Z_f} + \frac{|\boldsymbol{V}_{\mathrm{FEC},a}|}{3R_{\mathrm{PE}} + R_f}. \tag{5}$$

The module of the current as a function of the alternative component of the FEC voltage given in Eq. (5) is shown in Fig. 2.

From the analysis of the figure, it is clear that, to minimize the FEC current, the resistance of the protection wire must be higher than the minimum value,

$$R_{\mathrm{PE}} > \frac{Z_f}{3}, \tag{6}$$

and the alternate component of the FEC voltage must be equal to the

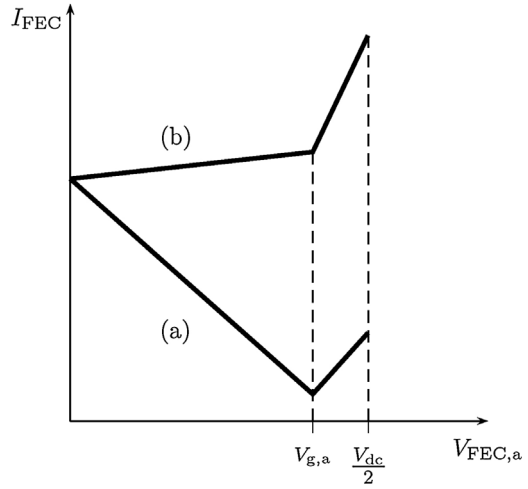

Fig. 2. FEC current versus alternative component of the FEC voltage: (a) $R_{PE} > Z_f/3$; (b) $R_{PE} < Z_f/3$.

grid voltage.

Summarizing, when a fault is detected, the converter starts generating voltage whose fundamental component is equal to the grid voltage. Then, it partially compensates the zero-sequence component using the residual voltage to reach the limit of the linear modulation. This is clearly explained in Fig. 3.

Anyway, in order to stabilize the control system and have it not affected by measurement errors, a closed-loop implementation of the control strategy is preferred. The aim of the control is to set to zero the alternating current flowing in the converter. For this reason, the easier implementation consists in setting to zero the direct and quadrature reference current. Using a traditional control on a Park reference frame, the sinusoidal modulating signal for the three phase voltages can be obtained [30]. In order to partially compensate the zero-sequence current, a continuous value is added to the sinusoidal modulating signals, making them saturate to one according to Fig. 3. The control scheme is depicted in Fig. 4.

The fault detection can be actuated looking at the zero-sequence of the current. When the zero-sequence of the current becomes higher than a fixed threshold, the fault is identified. The choice of a correct threshold is important to avoid false trips. Indeed, it is important to take into account that a zero-sequence of the current can circulate in the capacitance versus ground of the cables of the dc grid. For this reason, the threshold must not be too small. It has been experimentally verified that a threshold around 1% of the rated current can be a good value to avoid false trips and to achieve a fast intervention.

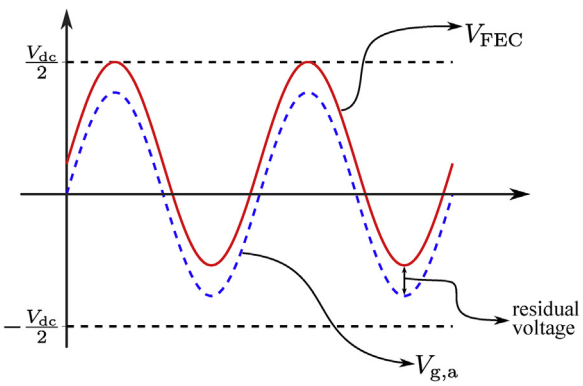

Fig. 3. Fundamental component of the phase grid voltage (dashed blue line) and phase FEC voltage (solid red line).

2.3. Selectivity and continuity of service

In this work, the selectivity and continuity of service are obtained resorting to a completely decentralized protection structure that does not require a communication level. In this way, it is possible to increase the reliability of a system that is robust against the problems related to communications, e.g., time delay, and also reduce the final cost and the complexity of the dc microgrid. To achieve these goals, the control strategy of the FEC is integrated with differential breakers installed on the feeders of the LVDC grid and with systems, e.g., ESS, able to supply the grid during the fault. The implementation of the discussed control strategy allows the limitation of the FEC current. In particular, the choice of correct resistance for the protection wire ensures that the current is limited to a value that the FEC can supply. Let I_{max} be the maximum current that the FEC can supply during the time necessary to clear the fault; from Eq. (5) it results in

$$R_{PE} \geq \frac{V_{g,a}}{3I_{max}}. \tag{7}$$

It is worth noting that Eq. (7) has been obtained from Eq. (5) by imposing that the alternating component of the FEC is equal to the alternating component of the grid ($\boldsymbol{V}_{FEC,a} = \boldsymbol{V}_{g,a}$) and neglecting R_f, which, in turn, leads to a more conservative condition. Respecting Eqs. (6) and (7) allows the correct working of the FEC. Anyway, during this working condition, the FEC does not transfer active power to the dc grid and provides only the zero-sequence current to the fault. For this reason, it is necessary that, on the dc grid, some devices are able to supply the loads and the fault in order to keep the voltage at a level that is enough to allow the correct operation of the FEC. This function can be performed by a storage system correctly sized and well controlled.

In order to interrupt the fault current, it is essential to identify the feeder affected by the fault and isolate it. Being the current limited by the protection wire resistance and control of the converter, as a result the maximum current protection cannot be used. Regardless, the faulty feeder will be the only one for which the sum of the positive and negative pole currents is not null. For this reason, a differential protection is capable of identifying the fault. Equipping all the feeders with differential protections, e.g., the one discussed in [31], is enough to ensure the interruption of the faulty current. It is necessary that both poles are open to avoid a possible closure path for the fault current. When the faulty feeder is isolated, the zero-sequence component of the FEC current drops to zero, and the FEC automatically returns to normal working condition. It is worth noting that, during the fault, all the feeders (with the only exception of the one in which the fault effectively occurs) have been continuously supplied by the storage unit. This storage unit can be installed in different ways. It could be a centralized storage unit close to the FEC, or it could be a distributed storage system installed on each feeder after the breaker. If the distributed storage system configuration is used, it is possible to ensure continuity of service also to the faulty feeder. Indeed, after opening the breaker, the feeder can be supplied by the storage unit, and there is no closure path for the ground current. The fault, of course, must be cleared before reclosing the breaker; moreover, during this time, only the storage unit and, eventually, some local generators can feed the faulty feeder.

3. RSE dc microgrid system configuration

The configuration of the dc microgrid realized in RSE, in collaboration with the Department of Electronic, Information and Bioengineering of the Politecnico di Milano, is shown in Fig. 5. A photograph of the dc microgrid is shown in Fig. 6. The LVDC network is unipolar with a nominal voltage level of 380 V and operated as an ungrounded IT system.

The LVDC is supplied from a low-voltage ac (LVAC) grid through a 400 V/200 V Dy11 transformer via a bidirectional ac/dc FEC with a rated power of 100 kVA. The FEC participates in the regulation of the

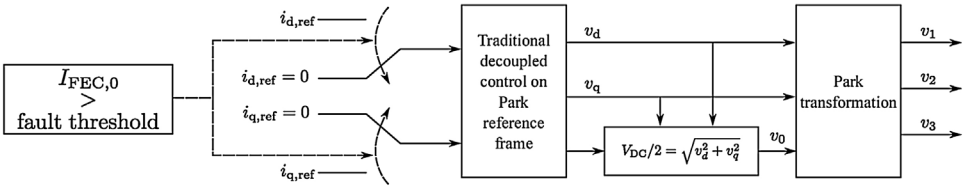

Fig. 4. Control scheme during fault operation.

dc network voltage and allows power flow from the ac to dc grid.

The network has also been equipped with different ESS units to ensure stabilization of the dc voltage during transient and at a steady state for different loads, both in ac grid-tie condition and in dc island operation. The ESSs are composed of two high-temperature SoNick batteries, each with a rated power of 32 kW, a capacity of 64 Ah, and a nominal voltage of 279 V, along with two supercapacitor (SC) banks, each with a rated power of 30 kW for 10 s and a maximum voltage of 384 V. Each battery and supercapacitor bank are coupled to the dc grid through a 35 kW dc/dc bidirectional converter to allow charge and discharge. Finally, two programmable purely resistive load-banks with a maximum power of 30 kW and adjustable with step changes of 1 kW, are installed in the dc microgrid. A summary of the main parameters of the dc microgrid is presented in Table 1.

The control strategy implemented in the overall dc grid should ensure stabilization of the dc voltage, the automatic configurability of the control scheme if one or more devices are unavailable, the self-recharge of the ESS, and the finest use of all of the devices. To achieve these goals, in all the converters connected to a source (FEC, ESSs, and SCs) a voltage control is implemented resorting to three control laws with different dynamic responses in accordance with [32]. Therefore, the closed-loop bandwidth of the converters is tuned and coordinated to achieve optimal use of the devices and, at the same time, to guarantee stabilization of the dc bus voltage. The stiff regulation of the dc voltage has been assigned just to the FEC to avoid continuous power flow from one converter to another, even in the absence of load or generation. The battery and supercapacitor converters contribute instead to voltage regulation, with a faster response, in order to supply power during transients. Therefore, the power supplied by the FEC is the smoothest possible, feeding only the mean power request from the dc grid, while the supercapacitors supply power during transients of a few seconds, and the batteries work at time periods ranging from a few seconds to some minutes.

In addition, for the ESS and SC converters, a state of charge (SoC)-based droop control [32] is implemented to allow the self-recharge of the supercapacitors and the batteries around the desired SoC value. This is achieved changing the dc voltage reference as a function of the actual SoC and the desired SoC.

The main parameters of the converters involved in the microgrid are reported in Tables 2 and 3 . The control structure of each converter and the regulator parameters are the same as presented in [32].

Fig. 6. Photo of the RSE dc microgrid.

Table 1
ac/dc microgrids characteristic data.

LVAC phase-to-phase voltage, V_{GRID}	400 V
LVAC frequency, f_{GRID}	50 Hz
ac cable resistance, R_s	8 mΩ
ac cable inductance, L_s	13 μH
dc nominal voltage, V_{dc}	380 V
Batteries nominal energy, E_b	17.8 kWh
Batteries nominal voltage, V_b	279 V
Supercapacitors capacitance, C_{SC}	4.58 F
Supercapacitors maximum voltage, V_{SC}^{max}	384 V
dc load maximum power, P_{load}^{max}	30 kW

Table 2
FEC converter parameters.

Transformer nominal power, S_n	100 kVA
Phase-to-phase winding voltages, V'_g/V_g	400 V / 200 V
Transformer connection	Dyn
Impedance voltage, V_{sc}%	12%
Load losses, P_{sc}%	1.5%
FEC nominal power, P_{FEC}	100 kW
FEC Incoming filter inductance, L_{in}	63 μH
FEC Incoming filter capacitance, C_{in}	100 μF
FEC dc-link capacitance, C_{dc}	20.4 mF
FEC Switching frequency, f_{FEC}^{sw}	5 kHz

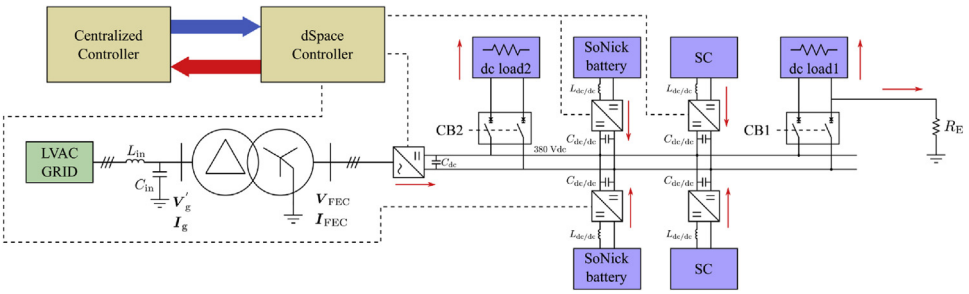

Fig. 5. Layout of the dc microgrid at RSE. Red arrows show the convention for the positive flow of powers for FEC, supercapacitors, SoNick batteries, loads, and fault. (For interpretation of the references to color in this legend, the reader is referred to the web version of the article.)

Table 3
dc/dc converter parameters.

DC/DC converter nominal power, $P_{dc/dc}$	35 kW
DC/DC converter capacitances, $C_{dc/dc}$	6.8 mF
DC/DC converter inductances, $L_{dc/dc}$	1.12 μH
DC/DC switching frequency, $f^{sw}_{dc/dc}$	4 kHz

4. Experimental and simulation results

Simulations and experimental verification have been designed to validate the effectiveness of the proposed approach and to demonstrate the ability of the control strategy to detect the fault and automatically isolate the faulty feeder without affecting operation of the whole system. Both in simulation and in the real microgrid, the test is conducted starting from a steady-state condition, with the two load feeders supplied by the FEC converter, and introducing a positive pole-to-ground fault. Similar results can be achieved also with a negative pole-to-ground fault with the only difference on the direction of the current and the bridge diodes that conduct [11]. The simulation and the test on the real dc microgrid are performed with the worst possible fault resistance (dead short with $R_g = 0\ \Omega$) and resorting to two different PE intentional resistances R_{PE}. This is done to avoid damage on the real dc microgrid. The total fault loop resistance $\hat{R}_g$ can be regarded as an equivalent resistance resulting from the sum of PE intentional resistance R_{PE} and the real fault resistance R_g. In the case of a fault, the differential protection of the faulty feeder isolates it from the dc microgrid, after a definite tripping delay, and also upon attempting to reclose the feeder after another defined delay time. The test case conditions are summarized in Table 4.

4.1. Simulations

Simulations were carried out on the model of the dc microgrid presented above, resorting to simple battery and supercapacitor models, because it has no impact on the simulation results. The following sequence of events is simulated:

- at $t = 0.2$ s, on FEEDER 1 a short circuit between the positive dc line and the PE conductor occurs;
- at $t = 0.25$ s, the breaker CB1, measuring a residual current, opens, and the FEEDER 1 is disconnected from the dc bus;
- at $t = 0.4$ s, the breaker CB1 tries an automatic reclosure, but the fault has not been cleared;
- at $t = 0.45$ s, the breaker CB1 measuring a residual current, opens again, and the FEEDER 1 is disconnected from the dc bus;
- at $t = 0.5$ s, the fault is cleared;
- at $t = 0.6$ s, the breaker CB1 tries an automatic reclosure; being the fault cleared, the microgrid starts to operate normally.

Protection control of the FEC is activated when a zero-sequence component in the three phase currents at the ac side is detected. When it occurs, FEC control is activated. In this way, as described in Section 2, the FEC stops feeding the loads, and its task is switched to zero-sequence current controlling. FEC's switching components do not have to sustain a dangerous current, and this operation method could last indefinitely, being limited only by the finite capacitance of the installed storage devices. In fact, they now must feed dc loads and ground faults. Simultaneously, bipolar protection switches—which continuously check the presence of zero-sequence component of the currents in the feeder—sense either one of the following cases:

1. no zero-sequence component;
2. presence of zero-sequence component.

The former situation reveals that the feeder is not affected by the ground fault, and, thus, that switches must not trip. On the other hand, the latter reveals the presence of a ground fault in the feeder. In this case, switches must trip. When switches trip, the zero-sequence component in the ac-side currents is eliminated. Thus, FEC automatically restores its normal operation.

After a predefined delay (in this case study, a delay of 150 ms has been set), the switch of the faulty feeder can try to reclose in order to check if a temporary fault has occurred and to preserve quality of supply of the feeder. If the fault has been cleared, no further zero-sequence component is detected, and effective normal operation can be guaranteed to the whole system. If the fault has not been cleared, a zero-sequence component is again detected and the above-described procedure starts. The number of reclosing attempts depends on the management criteria of the microgrid.

It is worth noting that both poles of the feeders must be opened. In fact, if only one pole of the faulty dc feeder is opened by the circuit breaker, there will be a reclosing path for the ground fault current. Thus, the presence of only one pole circuit breaker would be totally ineffective in the case of ground fault.

Fig. 7 shows the trend of the three legs FEC currents during the simulation. Note that, when ground fault is detected and before the tripping of the circuit breakers of FEEDER 1 (i.e., $0.2\ \text{s} \le t \le 0.25\ \text{s}$), the currents flowing through the FEC have only a zero-sequence component (with the exception of high-frequency ripple). Because the three legs of the FEC are in parallel for the zero-sequence current, only one-third of the fault current flows in each converter leg. When FEEDER 1 is disconnected by CB1 intervention, FEC starts normal operation. Then, at $t = 0.4$ s, circuit breakers of FEEDER 1 try to reclose. Because the fault is still present, the FEC only provides the zero-sequence current. Moreover, CB1 feeling the zero-sequence current opens again at $t = 0.45$ s. The next reclosing attempt, at $t = 0.6$ s, finds a healthy feeder, and normal operation starts again. The current provided by the FEC is used to recharge the supercapacitors.

Fig. 8 shows the trend of dc bus voltage. During the fault, the storage units are capable of keeping the dc voltage at a level high enough to make the system work.

After the disconnection or the clearing of the fault, the dc voltage is restored to its rated value. The restoring of dc voltage after the second fault is not already completed at the end of the simulation. This depends on the necessity of recharging the supercapacitors, as will be clear after analysis of the powers exchanged by each device with the dc bus. In Fig. 9 depicts the dc currents supplied by the FEC to the positive and negative poles of the dc grid.

It can be seen that, during the fault, the two currents supplied by the FEC to the dc poles are both positive. It implies that the storage units are providing a closing path for the fault current. This is the reason why the breaker has to interrupt both positive and negative poles to clear the fault. In Fig. 10, the powers supplied (or absorbed) by each unit connected to the dc bus are reported.

As shown in Fig. 10, during the fault the power is supplied, essentially, by supercapacitors. The continuous component of the current supplied by the FEC implies a power transfer because of the presence of a limited zero-sequence component of voltage according to Eq. (4). The intervention of batteries is limited because of the short time of

Table 4
Test case data.

	Simulation	Experimental test
DC voltage, V_{dc}		380 V
Supercapacitors initial voltage, V_{SC}		220 V
Batteries initial voltage, V_b		272 V
DC load resistances, $R_1 = R_2$		20 Ω
Fault resistances, $R_{PE} + R_g$	0.5 Ω	5 Ω
Circuit breaker tripping delay	0.15 s	3 s
Delay time before circuit breaker reclosing	0.15 s	20 s

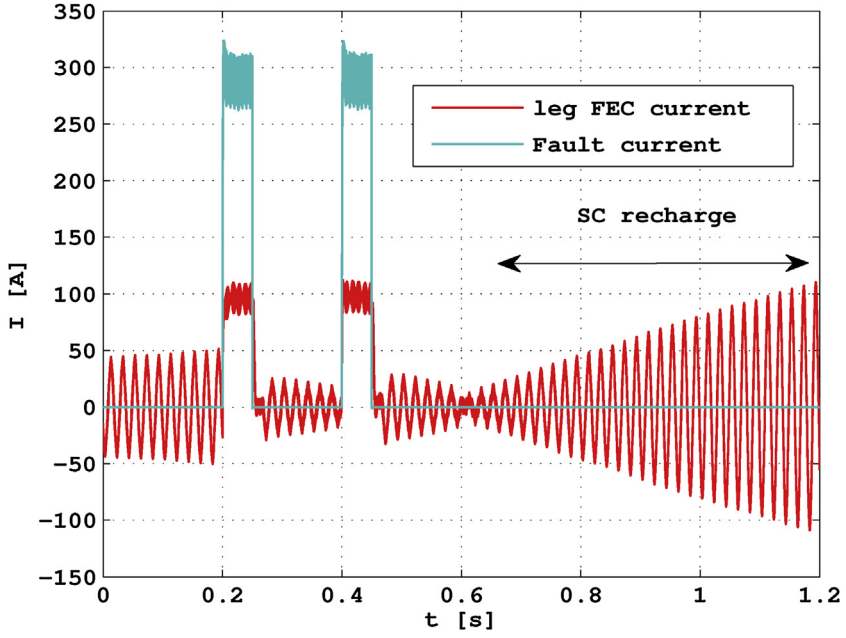

Fig. 7. Fault current and its impact on one leg's FEC current. (For interpretation of the references to color in this legend, the reader is referred to the web version of the article.)

simulated transients, but they practically supply almost all the power required by the loads. Their dynamic behavior is limited by the control of their boost converter. After fault clearance, the FEC supplies a power higher than the load request because supercapacitors need to be recharged. In order to be recharged, the supercapacitors keep the dc voltage at a level lower than the rated one, which is in agreement with the control of the system presented in Section 3.

4.2. Experimental results

The same two cases considered in the simulations have been taken into account in order to validate the effectiveness of the proposed control strategy, through experimental activity in the RSE test facility. The PE intentional resistance R_{PE} is equal to zero, while the ground fault resistance R_g between the positive pole of the dc bus of FEEDER 1 and ground is about 5 Ω. The two loads have a power of 8 kW. The ground fault occurs at time 5 s and, after a predefined delay of 20 s, the switch of the faulty feeder can try to reclose in order to check whether or not the fault has been cleared and to preserve quality of supply of the feeder. If the fault has been cleared (CASE 1), no further zero-sequence component is detected, and effective normal operation can be guaranteed to the whole system. If the fault has not been cleared (CASE 2), a zero-sequence component is again detected, and the above-described procedure starts.

Fig. 11 shows the trend of the rms at 50 Hz and the dc component of FEC leg current in CASE 1.

Note that, when ground fault is present and before the tripping of the circuit breakers of FEEDER 1 (i.e., 5 s $\leq t \leq$ 8 s), the current flowing

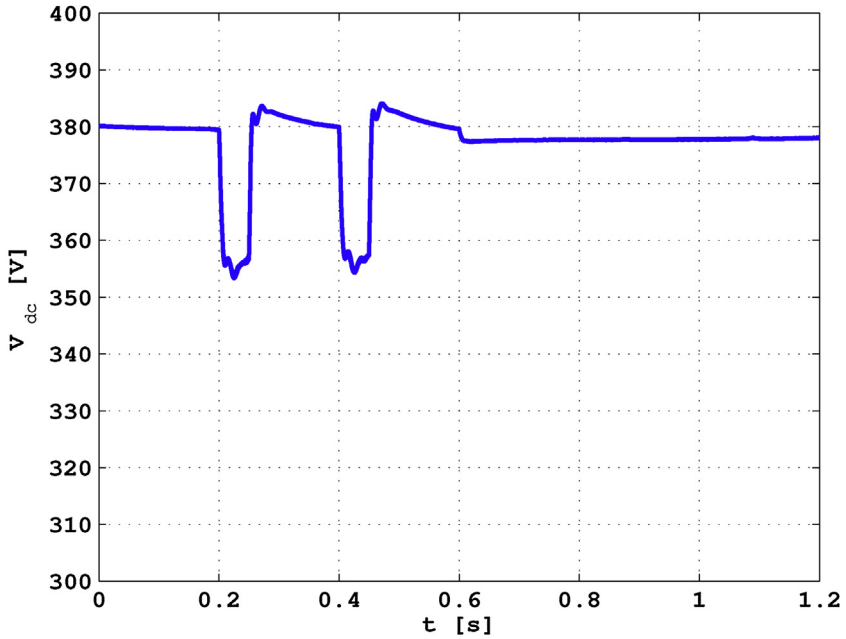

Fig. 8. Impact of a line-to-ground fault on the LVDC voltage.

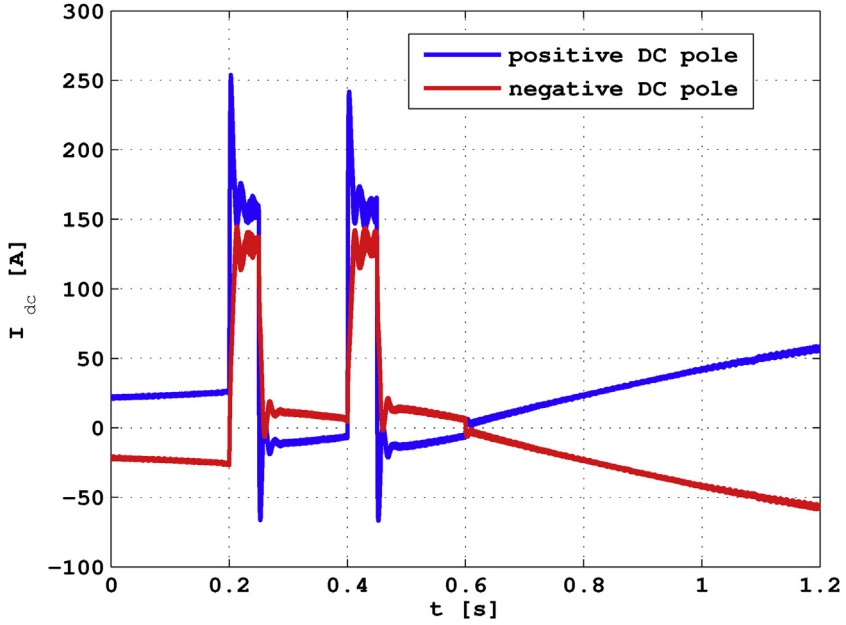

Fig. 9. Impact of a line-to-ground fault on FEC currents supplied to dc poles. (For interpretation of the references to color in this legend, the reader is referred to the web version of the article.)

through the FEC leg has only a zero-sequence component. When FEEDER 1 is disconnected, FEC starts normal operation. Due to the control strategy implemented in the overall dc grid described in Section 3, the dynamic of the FEC current, after opening the switch, has an oscillatory trend due to the recharge of supercapacitors and batteries, as shown in Fig. 13. Then, at 28 s, circuit breakers of FEEDER 1 succeed in reclosing because the ground fault has been cleared. From now on, FEC starts feeding also the load of FEEDER 1.

Fig. 12 shows the trend of dc bus voltage. After the transient, dc bus voltage is restored to the nominal value.

During the fault, the dc bus voltage is maintained to the reference voltage by supercapacitor and battery converters. Fig. 13 shows the power delivered by each converter, load power, and fault power.

Before the occurrence of fault and after fault clearance, the load is supplied by the FEC, while the energy storage systems give no contribution. During the fault, the active power feeding by the FEC reaches zero, and the load is supplied by a supercapacitor and battery. After tripping the circuit breakers of FEEDER 1 ($t > 8$ s), the FEC provides the power requested by the remaining load. When the fault has been cleared, FEC starts feeding also the load of FEEDER 1.

On the other hand, Fig. 14 shows the rms at 50 Hz and the mean component of the FEC leg current when the ground fault is not cleared and the reclosing attempt does not succeed.

In this case, FEEDER 1 must be permanently disconnected until the fault is cleared.

Fig. 15 shows how dc bus voltage is affected during an ineffective

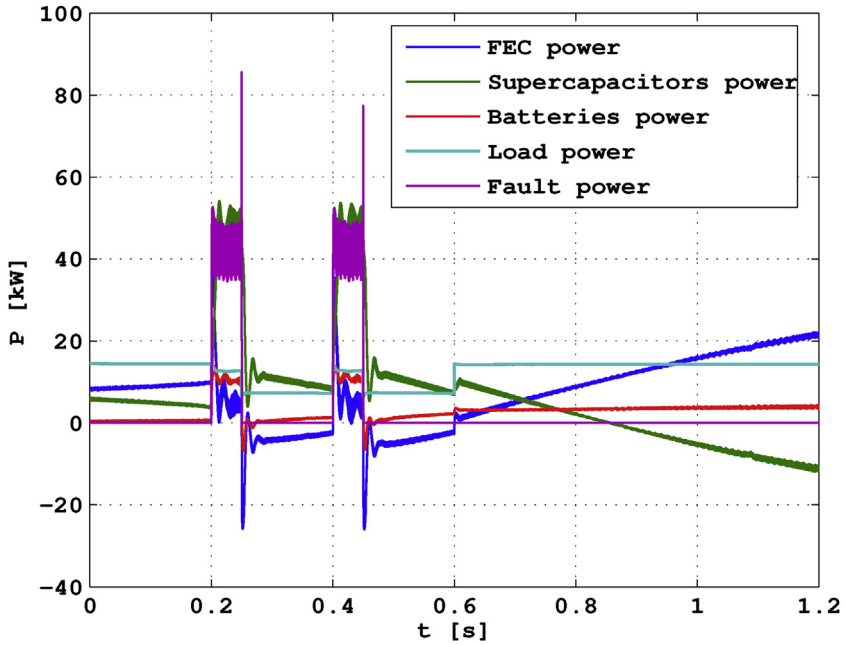

Fig. 10. Power supplied by the different devices to the LVDC microgrid. Sign convention is according to the red arrows in Fig. 5. (For interpretation of the references to color in this legend, the reader is referred to the web version of the article.)

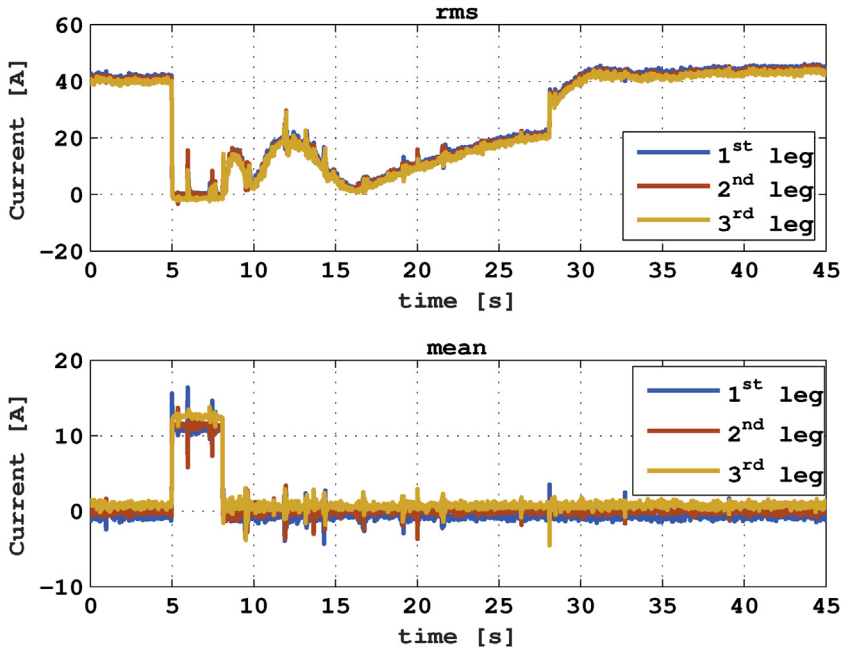

Fig. 11. Impact of a line-to-ground fault on FEC currents (rms and dc components) during test CASE 1 (i.e., with fault clearance). (For interpretation of the references to color in this legend, the reader is referred to the web version of the article.)

reclosing procedure.

Fig. 16 shows the power delivered by each converter, load power, and fault power.

Note that the proposed control strategy guarantees selectivity and a high security level. In fact, on the one hand, the presence of storage devices allows for complete load supply before the fault clearance; on the other hand, only the faulty feeder is permanently disconnected (if the fault is not cleared). In this way, only customers connected to the faulty feeder will undergo an outage but only for permanent ground faults. Indeed, after the switch trip also the loads connected to the faulty feeder may be supplied—until its complete depletion—by the connected storage device. Moreover, by knowing which circuit breaker has tripped, fault location would be eased.

5. Conclusion

This paper proposes a methodology for guaranteeing selectivity and security of a dc microgrid. This methodology is based on the fact that, when a ground fault is detected, the FEC stops supplying the load and starts sustaining the passage of the zero-sequence fault current. Each circuit breaker checks if the sum of the positive-pole and negative-pole current is different from zero and, in this case, opens the feeder, thus interrupting the closing path of the fault current. In this way, only this feeder is disconnected, while the others continue to be fed by storage devices. Further, the loads of the faulty feeder may be fed by (potentially present) local storage devices, until either fault clearance or complete depletion of the storage devices. When the ground fault is

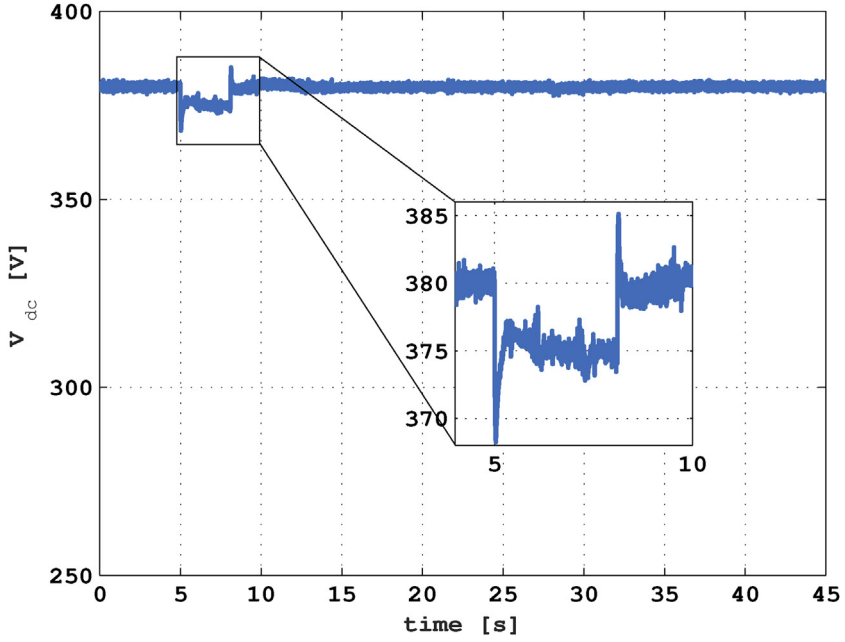

Fig. 12. Impact of a line-to-ground fault on the LVDC bus voltage during test CASE 1 (i.e., with fault clearance).

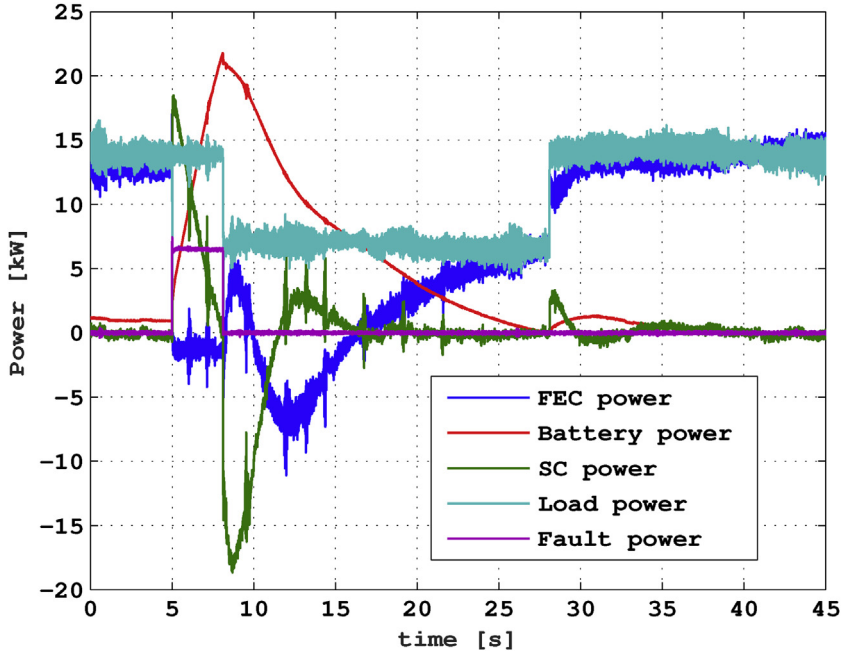

Fig. 13. Power supplied by the different devices to the LVDC microgrid during test CASE 1 (i.e., with fault clearance). (For interpretation of the references to color in this legend, the reader is referred to the web version of the article.)

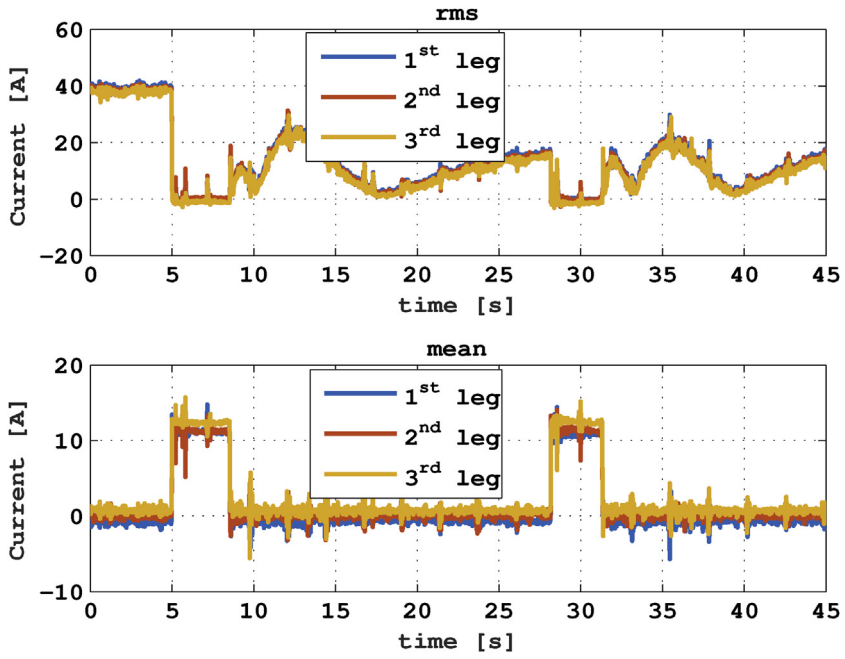

Fig. 14. Impact of a line-to-ground fault on FEC currents (rms and dc components) during test CASE 2 (i.e., without fault clearance). (For interpretation of the references to color in this legend, the reader is referred to the web version of the article.)

cleared (either by the permanent trip of the feeder's circuit breakers or by autonomous clearance), FEC operation can be restored to normal operation condition.

This protection scheme has been implemented on a real microgrid realized in RSE. It is a dc microgrid, equipped with two different storage systems (i.e., SoNick batteries and supercapacitors) and two separate resistive loads. Each load is connected to the dc bus through a two-pole circuit breaker. In order to check the behavior of the protection scheme, simulations have been preventively performed. The same scenarios, but with a different time scale, have been tested on the real grid. Measurements show that, by combining the presence of energy storage systems with a resistance in series with the PE conductor, a specifically designed control scheme for the FEC, and a protection logic for the circuit breakers, both selectivity and security of a dc microgrid can be guaranteed.

Acknowledgment

This work was financed by the Research Fund for the Italian Electrical System under the Contract Agreement between RSE S.p.A. and the Ministry of Economic Development – General Directorate for Nuclear Energy, Renewable Energy and Energy Efficiency in compliance with the Decree of March 8, 2006.

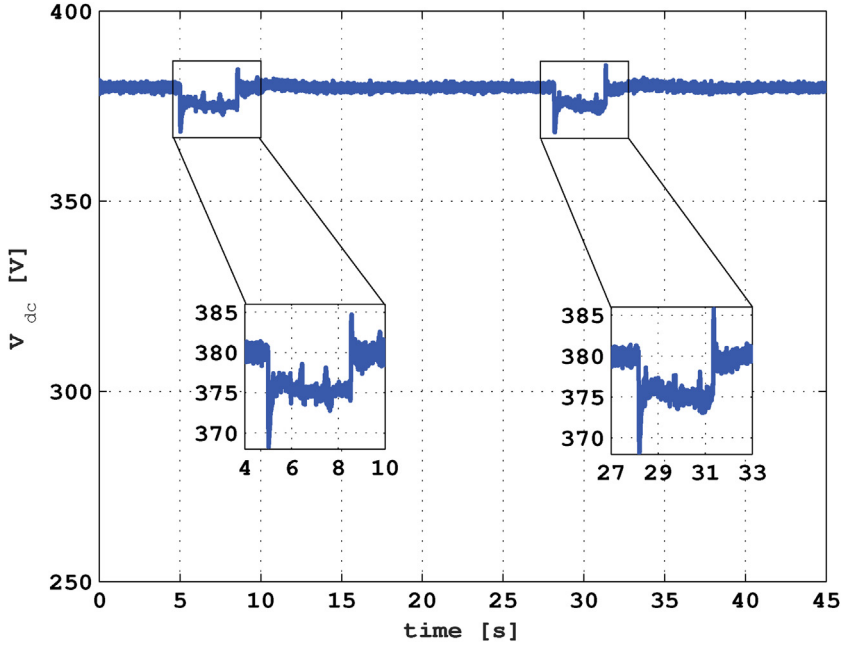

Fig. 15. Impact of a line-to-ground fault on the LVDC bus voltage during test CASE 2 (i.e., without fault clearance).

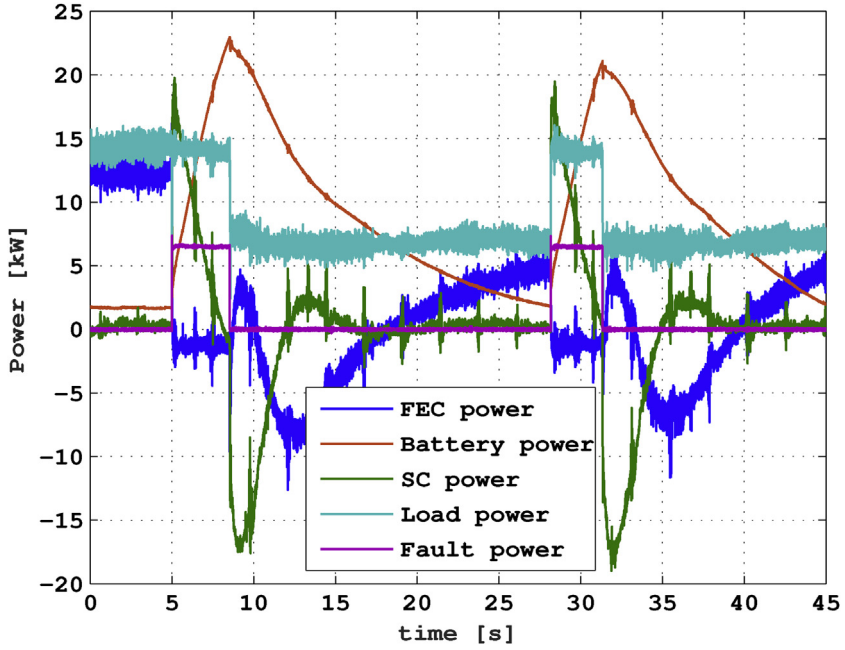

Fig. 16. Power supplied by the different devices to the LVDC microgrid during test CASE 2 (i.e., without fault clearance). (For interpretation of the references to color in this legend, the reader is referred to the web version of the article.)

References

[1] P. Salonen, T. Kaipia, P. Nuutinen, P. Peltoniemi, J. Partanen, An LVDC distribution system concept, Nordic Workshop on Power and Industrial Electronics (2008) 1–7.

[2] M. Brenna, C. Bulac, G.C. Lazaroiu, G. Superti-Furga, E. Tironi, DC power delivery in distributed generation systems, IEEE International Conference on Harmonics and Quality of Power (2008) 1–6.

[3] A. Agustoni, E. Borioli, M. Brenna, G. Simioli, E. Tironi, G. Ubezio, LV DC distribution network with distributed energy resources: analysis of possible structures, 18th International Conference and Exhibition on Electricity Distribution (CIRED), IET (2005) 1–5.

[4] D. Salomsson, A. Sannino, Low-voltage DC distribution system for commercial power systems with sensitive electronic loads, IEEE Trans. Power Del. 22 (3) (2007) 1620–1627.

[5] M. Brenna, E. Tironi, G. Ubezio, Proposal of a local DC distribution network with distributed energy resources, IEEE International Conference on Harmonics and Quality of Power (2004) 397–402.

[6] F. Sanchez-Sutil, J.C. Hernández, C. Tobajas, Overview of electrical protection requirements for integration of a smart DC node with bidirectional electric vehicle charging stations into existing AC and DC railway grids, Electr. Power Syst. Res. 122 (2015) 104–118.

[7] D. Salomsson, L. Soder, A. Sannino, Protection of low-voltage DC microgrids, IEEE Trans. Power Del. 24 (3) (2009) 1045–1053.

[8] P. Nuutinen, P. Peltonieni, P. Silventoinen, Short-circuit protection in a converter-fed low-voltage distribution network, IEEE Trans. Power Electron. 28 (4) (2013) 1587–1597.

[9] R.M. Cuzner, G. Venkataramanan, The status of DC micro-grid protection, IEEE Industry Applications Society Annual Meeting (2008) 1–8.

[10] Y. Wang, Z. Zhang, Y. Fu, Y. Hei, X. Zhang, Pole-to-ground fault analysis in transmission line of DC grids based on VSC, IEEE 8th International Power Electronics and Motion Control Conference (IPEMC-ECCE Asia) (2016) 2028–2032.

[11] J. Yang, J.E. Fletcher, J. O' Reilly, Short-circuit and ground fault analyses and location in VSC-based DC network cables, IEEE Trans. Ind. Electron. 59 (10) (2012)

3827–3837.
[12] S. Xue, F. Gao, W. Sun, B. Li, Protection principle for a DC distribution system with a resistive superconductive fault current limiter, Energies 8 (6) (2015) 4839–4852.
[13] M. Monadi, M.A. Zamani, J.I. Candela, A. Luna, P. Rodriguez, Protection of AC and DC distribution systems embedding distributed energy resources: a comparative review and analysis, Renew. Sustain. Energy Rev. 51 (2015) 1578–1593.
[14] M. Farhadi, O.A. Mohammed, Protection of multi-terminal and distributed DC systems: design challenges and techniques, Electr. Power Syst. Res. 143 (2017) 715–727.
[15] R. Dantas, J. Liang, C.E. Ugalde-Loo, A. Adamczyk, C. Barker, R. Whitehouse, Progressive fault isolation and grid restoration strategy for MTDC networks, IEEE Trans. Power Del. 33 (2) (2018) 909–918.
[16] D.M. Bui, S.L. Chen, C.H. Wu, K.Y. Lien, C.H. Huang, K.K. Jen, Review on protection coordination strategies and development of an effective protection coordination system for DC microgrid, Asia-Pacific Power and Energy Engineering Conference (2014) 1–10.
[17] C. Peng, A.Q. Huang, A protection scheme against DC faults VSC based DC systems with bus capacitors, 29th Annual Applied Power Electronics Conference and Exposition (2014) 3423–3428.
[18] G. Patil, M.F.A.R. Satarkar, Autonomous protection of low voltage DC microgrid, International Conference on Power, Automation and Communication (2014) 23–26.
[19] J.C. Hernández, F.S. Sutil, P.G. Vidal, Protection of a multiterminal DC compact node feeding electric vehicles on electric railway systems, secondary distribution networks, and PV systems, Turk. J. Electr. Eng. Comput. Sci. 24 (4) (2016) 3123–3143.
[20] M.E. Baran, N.R. Mahajan, Overcurrent protection on voltage-source-converter-based multiterminal DC distribution systems, IEEE Trans. Power Del. 22 (1) (2007) 406–412.
[21] G. Madingou, M. Zarghami, M. Vaziri, Fault detection and isolation in a DC microgrid using a central processing unit, Innovative Smart Grid Technologies Conference (2015) 1–5.
[22] A. Meghwani, S.C. Srivastava, S. Chakrabarti, A new protection scheme for DC microgrid using line current derivative, IEEE PES General Meeting (2015) 1–5.
[23] J.D. Park, J. Candelaria, Fault detection and isolation in low-voltage DC-bus microgrid system, IEEE Trans. Power Del. 28 (2) (2013) 779–787.
[24] B. Heinbokel, H. Kirchhoff, T. Dragicevic, Zonal protection of DC swarm microgrids using a novel multi-terminal grid interface with decentralized control, 50th International Universities Power Engineering Conference (2015) 1–6.
[25] J.C. Das, R.H. Osman, Grounding of AC and DC low-voltage and medium-voltage drive systems, IEEE Trans. Ind. Appl. 34 (1) (1998) 205–216.
[26] A. Medina, J.C. Hernández, M.J. Ortega, F. Jurado, DC current injection into the network from transformerless and LF transformer photovoltaic inverters, IEEE 16th International Conference on Harmonics and Quality of Power (ICHQP) (2014) 234–238.
[27] M. Carminati, E. Ragaini, S. Grillo, L. Piegari, E. Tironi, Ground fault analysis of low voltage DC micro-grids with active front-end converter, Renewable Power Generation Conference (2014) 1–6.
[28] L. Tang, B.-T. Ooi, Impact of zero sequence component on voltage source converters, Power Conversion Conference, vol. 1 (2002) 184–189.
[29] M. Nieves-Portana, M. Barragán-Villarejo, J.M. Maza-Ortega, J.M. Mauricio-Ferramola, Reduction of zero sequence components in three-phase transformerless multiterminal DC-link based on voltage source converters, International Conference on Renewable Energies and Power Quality (ICREPQ) (2013) 1206–1211.
[30] L. Piegari, P. Tricoli, A control algorithm of power converters in smart-grids for providing uninterruptible ancillary services, 14th International Conference on Harmonics and Quality of Power (ICHQP), IEEE (2010) 1–7.
[31] Abb Schweiz AG, DC grid protection method and system thereof, U.S. Patent WO2016/074199. (05 2016).
[32] S. Grillo, V. Musolino, L. Piegari, E. Tironi, C. Tornelli, DC islands in AC smart grids, IEEE Trans. Power Electron. 29 (1) (2014) 89–98.